Sensors and Actuators A 149 (2009) 298–304

Contents lists available at ScienceDirect

Sensors and Actuators A: Physical

journal homepage: www.elsevier.com/locate/sna

Investigation of Ni-based thermal bimaterial structure for sensor and actuator application

Chia-Sheng Huang[a], Yu-Ting Cheng[b], Junwei Chung[a], Wensyang Hsu[a,*]

[a] Department of Mechanical Engineering, National Chiao Tung University, 1001 Ta Hsueh Road, Hsinchu 300, Taiwan
[b] Department of Electronics Engineering, National Chiao Tung University, 1001 Ta Hsueh Road, Hsinchu 300, Taiwan

ARTICLE INFO

Article history:
Received 20 March 2008
Received in revised form
30 September 2008
Accepted 14 November 2008
Available online 30 November 2008

Keywords:
Bimaterial structure
Bimorph
Electroplating
Nanocomposite

ABSTRACT

Thermal bimaterial structures made of Ni and Ni-diamond nanocomposite for sensor and actuator application are proposed, fabricated, and tested. Two deflection types of thermal bimaterial structures, including upward and downward bending types, can be easily fabricated by controlling electroplating sequence of Ni and Ni-diamond nanocomposite. According to thermal performance measurement, the tip deflection of upward and downward types can reach about 82.5 μm and −22.5 μm for a temperature change of 200 °C, respectively. In the condition, the thermomechanical sensitivity and output force are 412.5 nm/K and 97.0 μN for upward type thermal bimaterial structure; and −112.5 nm/K and −26.5 μN for downward type one. Due to the low electroplating process temperature (~50 °C) for both Ni-based layers, diminutive pre-deformation of as-fabricated structure and strong interlaminar bonding strength are verified by SEM and vibrational test. The resonant frequency of the structure remains unchanged after 10^9 cycles.

1. Introduction

Bimaterial structure can provide thermally bended deformation due to the coefficient of thermal expansion (CTE) mismatch between two bonded materials, so-called bimorph effect [1,2]. Upon this effect, the bimaterial structure-based transducers can detect external stimulus of temperature change and provide temperature-driven output force simultaneously. To date, thermal bimaterial structure has been widely utilized in several microelectro-mechanical systems (MEMS) devices, such as thermal sensor [3], stress sensor [4], biological sensor [5], microvalve [6], pumping membrane [7], tilting micromirror [8], microrelay [9], microswitch [10], etc. Nevertheless, thermal bimaterial structure typically will exhibit initial deformation once the structure is released. This deformation is resulted by the residual thermal stress [11–13] induced in structural fabrication where structural materials have different CTE and process temperatures. Delaminating is also a common issue that may happen on the interlamination through large residual stress and low cohesive energy [14,15] to reduce the lifetime and reliability of thermal bimaterial structure. For a bimaterial structure, by arranging the low-CTE layer on top, thermal upward actuation can be achieved [16,17]. However, since metal usually has higher CTE comparing to nonmetal material, thermal upward actuation is difficult to achieve when the metal layer is deposited above the nonmetal layer [8–10,13]. Thus, further investigations in terms of material and process selection and structure design are still required for future applications of thermal bimaterial structure.

In recent researches, Teh et al. found that the incorporation of nano-diamonds in electrolytic Ni matrix to form Ni-diamond nanocomposite could reduce the film residual stress and render the film more compressively [18]. Besides, the nanocomposite could exhibit a higher CTE than that of electroplated Ni [19]. Therefore, this study will investigate the bimorph effect of Ni/Ni-diamond nanocomposite bimaterial and propose a newly thermal bimaterial microactuator by employing the advantages of Ni-diamond nanocomposite. It is our belief that the proposed thermal device using the Ni/Ni-diamond nanocomposite bimaterial would have better interfacial bonding strength and smaller residual thermal stress since Ni and Ni-diamond nanocomposite have different CTE but similar crystal structure and process temperature. By controlling plating sequence of Ni and Ni-diamond nanocomposite, the fabricated thermal bimaterial structure desired to have upward or downward bended deformation can also be easily achieved.

2. Bimaterial structure design

Fig. 1 shows the scheme of thermal bimaterial structures made of Ni/Ni-diamond nanocomposite bimaterial including upward and downward deflection types for bimorph effect investigation. Upon

* Corresponding author.
E-mail address: whsu@mail.nctu.edu.tw (W. Hsu).

0924-4247/$ – see front matter © 2008 Elsevier B.V. All rights reserved.
doi:10.1016/j.sna.2008.11.019

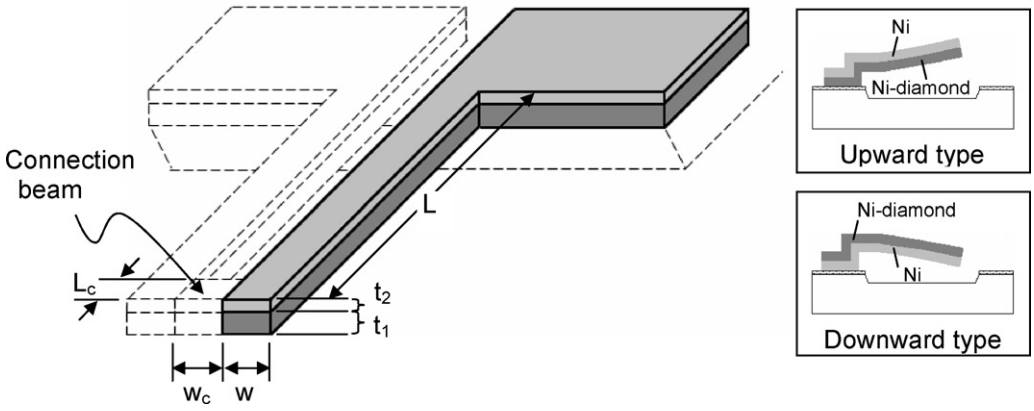

Fig. 1. Schematic illustration of Ni-based thermal bimaterial structures including upward and downward deflection types.

the plating sequence of Ni and Ni-diamond nanocomposite, two deflection types of thermal bimaterial structures, including upward and downward types, are available. The designed length L of fabricated thermal bimaterial structure ranged from 200 μm to 1500 μm where the width w is fixed at 50 μm. The connecting beam is 50 μm long (L_c) and 30 μm wide (w_c). The thickness of Ni and Ni-diamond nanocomposite layers are determined according to the optimum thermomechanical sensitivity S_T defined as tip deflection d for a temperature change ΔT:

$$S_T = \frac{d}{\Delta T} \tag{1}$$

where d and following F are the thermally generated tip deflection and the output force of a thermal bimaterial structure, respectively. The deflection and force can be expressed by the following equations [1]:

$$d = \frac{3w_1w_2E_1E_2t_1t_2(t_1+t_2)(\alpha_1-\alpha_2)\ \Delta TL^2}{(w_1E_1t_1^2)^2+(w_2E_2t_2^2)^2+2w_1w_2E_1E_2t_1t_2(2t_1^2+3t_1t_2+2t_2^2)} \tag{2}$$

and

$$F = \frac{3\overline{EI}d}{L^3} = Kd \tag{3}$$

where E_i, α_i, w_i, and t_i (i = 1, 2) are, respectively, Young's modulus, CTE, width, and thickness of each layer; L, $\overline{EI}$, and K are, respectively, the length, flexural rigidity and spring constant of thermal bimaterial structure, and ΔT is the temperature change.

A folded structure design is introduced into the thermal bimaterial structure to increase output force and to decrease the thermal vibrational noise. For thermal bimaterial structure, the amount of tip deflection is proportional to the square of the structure length as shown in Eq. (2), so the thermal bimaterial structure becomes more sensitive with increased length of bimaterial structure as shown in Eq. (1). However, lower spring constant resulting from an increased length also decreases the output force as shown in Eq. (3) and increases the thermal vibrational noise as follows [3]:

$$d_n = \sqrt{\frac{2k_BTB}{K\pi fQ}} \tag{4}$$

where k_B is the Boltzmann constant, T is the absolute temperature, B is the measurement bandwidth, K is the cantilever spring constant, f is the resonance frequency, and Q is the quality factor of the resonance. Since a folded structure behaves like the structure of two beams connected in parallel which can have a higher spring constant due to larger width, a promising way to increase output force and sensitivity of the thermal bimaterial structure without a significant increase of the thermal vibrational noise is to connect multiple bimaterial cantilever beams in a folded manner.

Before the layer thickness determination of thermal bimaterial structure, cantilevers made of single layer of Ni and Ni-diamond nanocomposite are first fabricated to characterize the CTE of material and to measure CTE mismatch. By measuring the elongation of cantilever in a heated chamber with temperature control, CTE of Ni and Ni-diamond nanocomposite are found to be $15.6 \times 10^{-6}/^{\circ}$C and $19.4 \times 10^{-6}/^{\circ}$C, respectively, where the diamond content of the corresponding nanocomposite film is 0.32% in weight fraction according to the elemental analyzer (EA) measurement. The Young's modulus of the electroplated film is characterized by the nanoindenter (MTS Nano Indentor XP) [20]. The indentation depth is set as 1/10 film thickness, and the measured value is the average over 20 test points. The measured Young's moduli of Ni and Ni-diamond nanocomposite by means of a nanoindentation test are found to be 211.0 GPa and 224.1 GPa, respectively.

Based on Eqs. (1) and (2) and aforementioned material properties, for the upward type thermal bimaterial structure with L = 1500 μm and w = 50 μm, the calculated thermomechanical sensitivity as function of Ni layer thickness and thickness ratio are shown in Fig. 2(a) and (b), respectively. Then, the optimal Ni thickness t_2 is found to be around half of the Ni-diamond nanocomposite thickness t_1 for the maximum themomechanical sensitivity [21]. For instance, for a bimaterial with the structure of 3 μm thick Ni and 6 μm thick Ni-diamond nanocomposite, the themomechanical sensitivity can be designed as high as 640.2 nm/K with the flexural rigidity of 6.61×10^{-10} N m^2, and the output force of 150.5 μN as ΔT = 200 °C. Similarly, for downward type thermal bimaterial structure, the layer thickness of Ni and Ni-diamond nanocomposite are also determined to be 3 μm and 6 μm, respectively.

3. Fabrication

Fig. 3 depicts the fabrication process of the proposed thermal bimaterial structure. Initially, the 0.5 μm thick SiO_2 on a silicon wafer with patterned etching windows is first coated with 5 μm thick AZP-4620 photoresist (PR) and patterned as sacrificial layer (Fig. 3(a)) After hard baking, it is followed by sputtering seed layer of 1000 Å Cu onto 200 Å Ti as adhesion layer. 15 μm thick AZP-4620 PR is then spin coated and patterned to form the plating mold of thermal bimaterial structure, as shown in Fig. 3(b). For upward type thermal bimaterial structure, the 6 μm thick composite-plating of Ni-diamond layer is deposited first to construct the bottom layer of thermal bimaterial structure. Subsequently, 3 μm thick electroplated Ni is deposited to construct the top layer (Fig. 3(c)). Table 1 shows the plating bath condition, and the plating temperatures of both layers are kept at 50 °C. For the composite-plating of Ni-

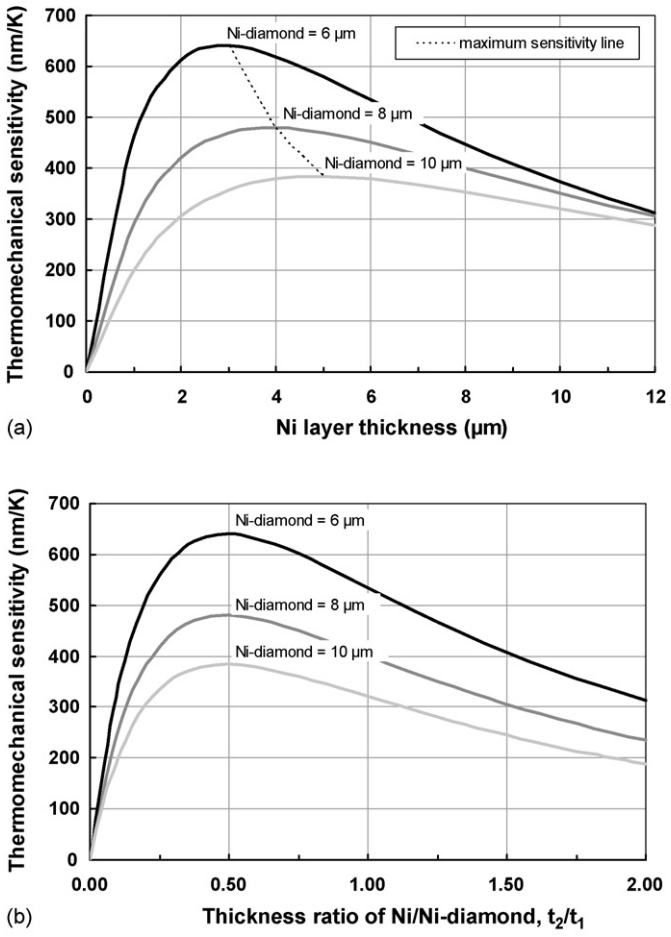

Fig. 2. (a) Calculated themomechanical sensitivity of thermal bimaterial structure for layer thickness determination; (b) The relationship between themomechanical sensitivity and thickness ratio of thermal bimaterial structure.

diamond nanocomposite which is different from electroplated Ni, the nano-diamond particles with 350 nm in average diameter are added into a sulfuric-based Ni plating bath for the co-deposition, and the concentration of the nano-diamond particles in plating bath is 2 g/L. Finally, the fabricated thermal bimaterial structure

Table 1
Plating bath conditions of Ni and Ni-diamond nanocomposite for structural layers of thermal bimaterial structure.

Electroplating: Ni	
Batch	
Nickel sulfamate (g/L)	400
Nickel chloride (g/L)	5
Boric acid (g/L)	40
Wetting agent (c.c.)	5
pH	4.1–4.3
Current density (mA/cm^2)	10
Temperature (°C)	50
Composite-plating: Ni-diamond nanocomposite	
Batch	
Nickel sulfamate (g/L)	400
Nickel chloride (g/L)	5
Boric acid (g/L)	40
Wetting agent (c.c.)	5
Concentration of diamond nanoparticles (g/L)	2
Diameter of diamond nanoparticle (nm)	~350
pH	4.1–4.3
Current density (mA/cm^2)	10
Temperature (°C)	50

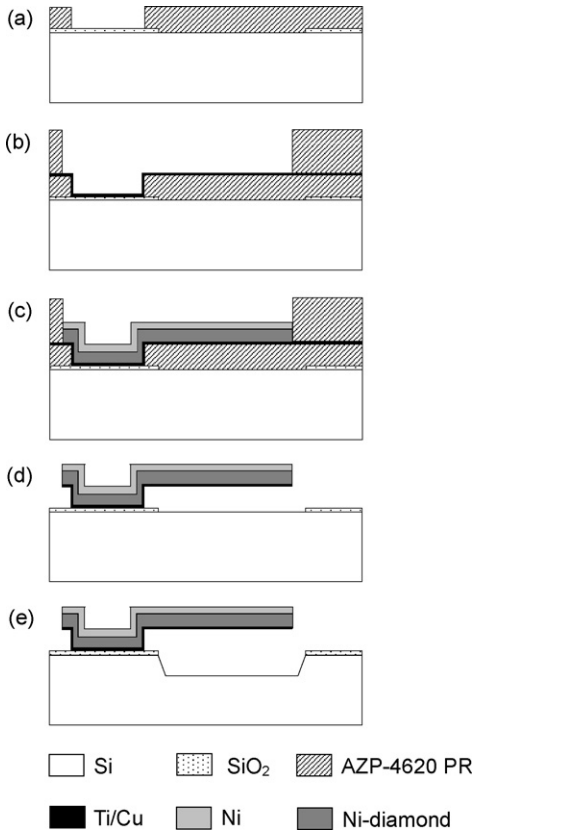

Fig. 3. Fabrication process of thermal bimaterial structure: (a) 5 μm AZP-4620 PR deposition and patterning; (b) sputtered Ti/Cu as an adhesion and seed layer, then 15 μm AZP-4620 PR deposition and patterning as the plating mold structure; (c) layers electroplating: Ni-diamond nanocomposite for bottom layer, and Ni for top layer (i.e. upward type); (d) structure releasing; (e) silicon removing by KOH.

is released after stripping the sacrificial layer by acetone solution (Fig. 3(d)), and the silicon underneath is removed by KOH solution (Fig. 3(e)). For downward type thermal bimaterial structure, the fabrication process is similar to the upward one except switching the plating sequence of Ni-diamond nanocomposite and Ni in Fig. 3(c). By controlling plating sequence of Ni and Ni-diamond nanocomposite, two deflection types of thermal bimaterial structures including upward and downward are easily fabricated.

Fig. 4(a) and (b) shows the scanning electron microscope (SEM) pictures of the upward and downward types of fabricated thermal bimaterial structures. It is found that no initial deformation is observed as proposed due to the same low process temperature of electrodeposited Ni and Ni-diamond nanocomposite for lower residual thermal stress in thermal bimaterial structure.

4. Measurements and discussions

4.1. Thermal performance measurement

Fig. 5 illustrates the set-up for the thermal performance measurement of the fabricated thermal bimaterial structure in terms of tip deflection in thermal chamber. First, a chip with thermal bimaterial structure is placed on a hot plate in a chamber with temperature controller, and the focused tip image of thermal bimaterial structure is captured by a charge-coupled device (CCD) through optical microscope with positional *z*-adjustment. As the thermal bimaterial structure is heated up, the structural tip will deflect and result in a focus change, which requires *z*-adjustment to search for a new focus to have a clear tip image. Thus, the micrometer-scale tip deflection of thermal bimaterial structure is determined by mea-

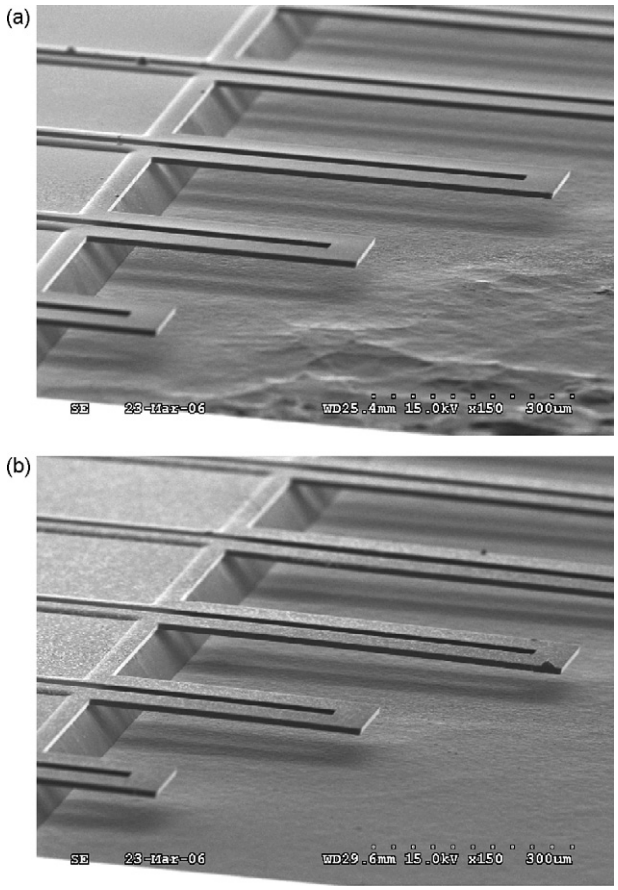

Fig. 4. SEM pictures of fabricated thermal bimaterial structures: (a) upward type: Ni layer on top of Ni-diamond nanocomposite layer; (b) downward type: Ni-diamond nanocomposite layer on top of Ni layer.

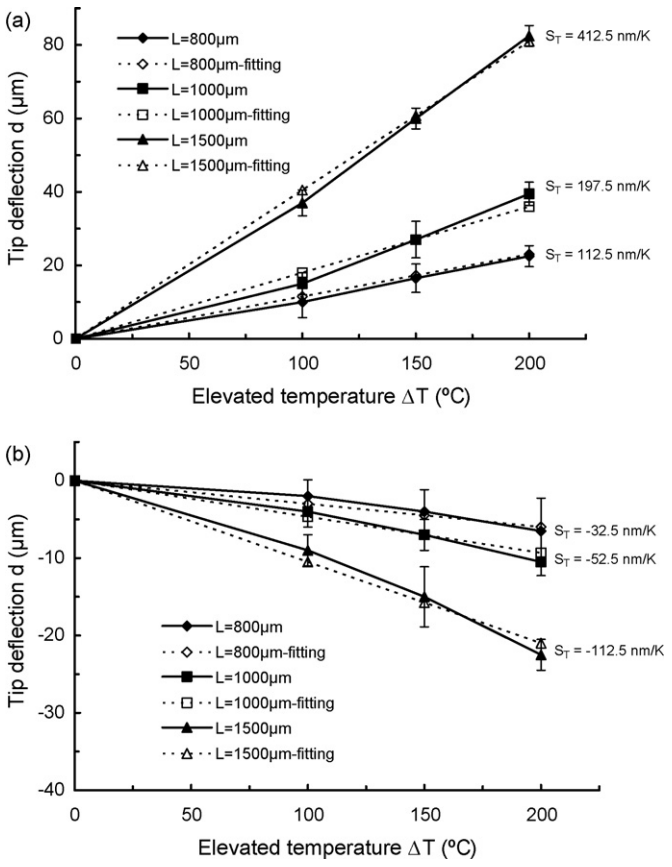

Fig. 6. Thermal performance measurement results and fitting curves in terms of the tip deflection of thermal bimaterial structure at elevated temperature: (a) upward type; (b) downward type.

suring the focus variation (ΔZ) and the measurement accuracy of ΔZ is about 0.5 μm on positional z-adjustment. The measured out-of-plane tip deflections of fabricated thermal bimaterial structures including upward and downward types with length of 800 μm, 1000 μm, and 1500 μm are observed with temperature change from 0 °C to 200 °C. The relationship between tip deflection and elevated temperature is plotted in Fig. 6(a) and (b). According to the measured results of thermal performance, as structure length L = 1500 μm and temperature change ΔT = 200 °C, the measured tip displacement of upward and downward types can reach around 82.5 μm and −22.5 μm, respectively. In this condition, the themomechanical sensitivity and output force are calculated, respectively, to be 412.5 nm/K and 97.0 μN for upward type thermal bimaterial structure; and −112.5 nm/K and −26.5 μN for downward type one.

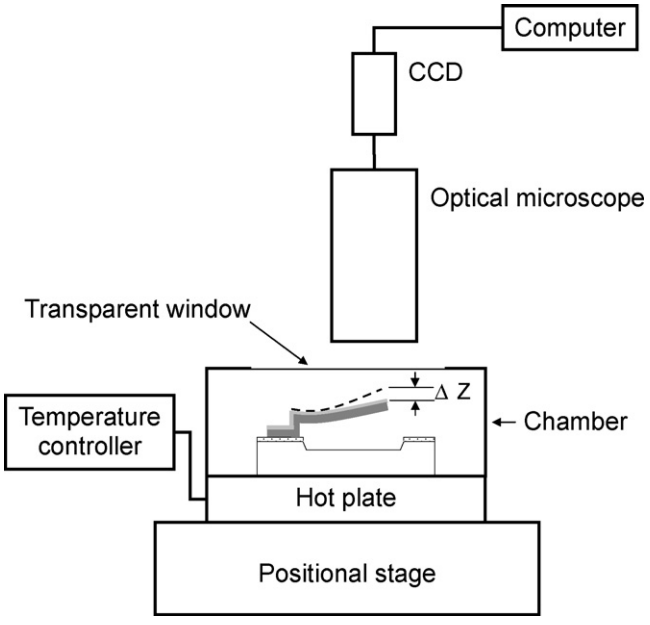

Fig. 5. Schematic diagram of set-up for thermal performance measurement of thermal bimaterial structure.

From above calculated results of upward type thermal bimaterial structure, the thermomechanical sensitivity and output force are smaller than the theoretical calculation; and the thermal performance in tip deflection of downward type is not as large as upward type. It seems that the CTE difference between Ni and Ni-diamond nanocomposite in the thermal bimaterial structure is not equal to the cantilevers' that made of single material layer. Assuming material properties of bottom structural layers of thermal bimaterial structure are the same as cantilever's that made of single Ni or Ni-diamond nanocomposite layer. Using Eq. (2) and the measured data of Fig. 6(a) and (b), the CTE of the top structural layer of thermal bimaterial structure have been modified to fit the experiment data. Therefore, the CTE of top structural layer of Ni in upward type is modified to be $16.9 \times 10^{-6}/°C$ which is 8.3% deviation from single Ni cantilever. Similarly, the CTE of top structural layer of Ni-diamond nanocomposite in downward type is modified to be $16.2 \times 10^{-6}/°C$ which is 16.5% deviation from single Ni-diamond nanocomposite cantilever.

Seed layer effect may be the major cause resulting in the aforementioned CTE variation. While Ni-diamond nanocomposite is

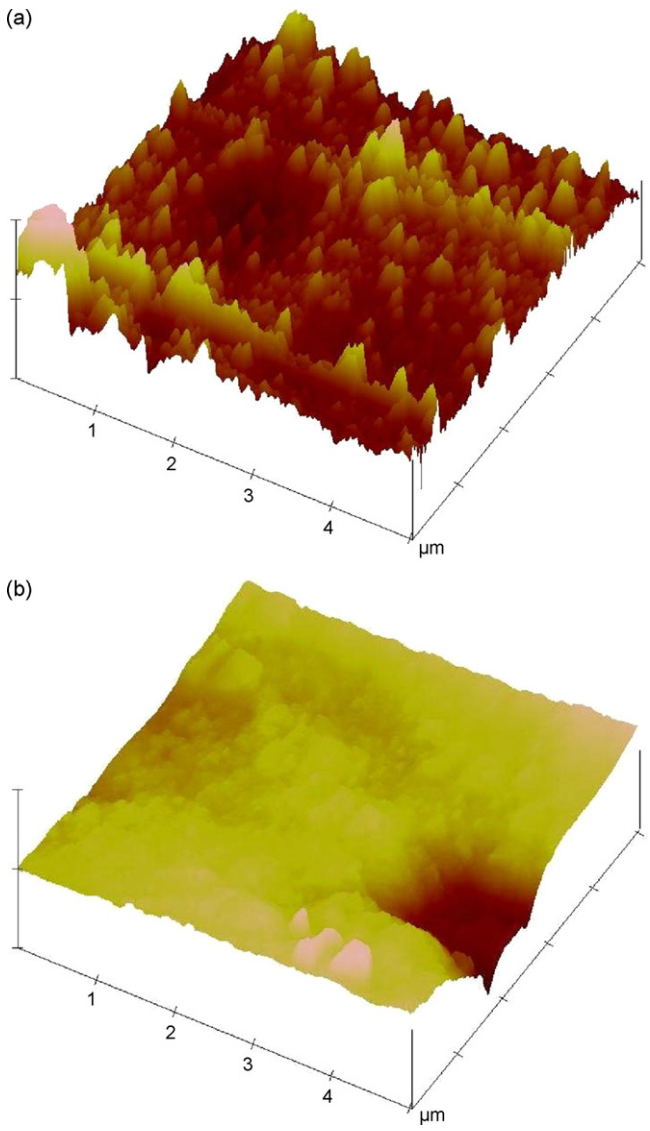

Fig. 7. AFM surface images of 6 μm Ni-diamond nanocomposite layer on the top of (a) 3 μm electroplated Ni layer, R_a = 15.313 nm; (b) 1000 Å sputtering Cu layer, R_a = 5.275 nm. *X*: 1 μm/div; *Z*: 200 nm/div.

used as the top structural layer of thermal bimaterial structure in downward type, the plating seed layer of Ni-diamond nanocomposite is a 3 μm thick electroplated Ni. On the contrary, as Ni-diamond nanocomposite is used as the bottom structural layer in upward type, the plating seed layer is 1000 Å sputtering Cu which is similar to single material cantilever. According to atomic force microscope (AFM) surface images of 6 μm Ni-diamond nanocomposite on 3 μm electroplated Ni and 1000 Å sputtered Cu seed layers as shown in Fig. 7(a) and (b), respectively, the Ni-diamond nanocomposite electroplated on the Ni layer has a higher surface roughness value (R_a) than that on the sputtering Cu layer. The rougher surface could be attributed to that grain structure difference of Ni-diamond nanocomposite that may vary with the different seed layers and so does the material property of CTE. Further material characterization is required for verification.

4.2. Interlaminar reliability test

Fig. 8(a) and (b) shows the side wall SEM pictures of two bimaterial structure types including upward and downward, respectively. Due to similar crystal structures of Ni-base between plating Ni and Ni-diamond nanocomposite, the outside interlaminar boundary of fabricated thermal bimaterial structure is not evident. Fig. 9 also shows the bright field transmission electron microscope (TEM) image of cross section of fabricated thermal bimaterial structure that the interface boundary displays strong bonding as similar Ni crystal structure. To further investigate the bonding strength, the following vibration test [22] is performed.

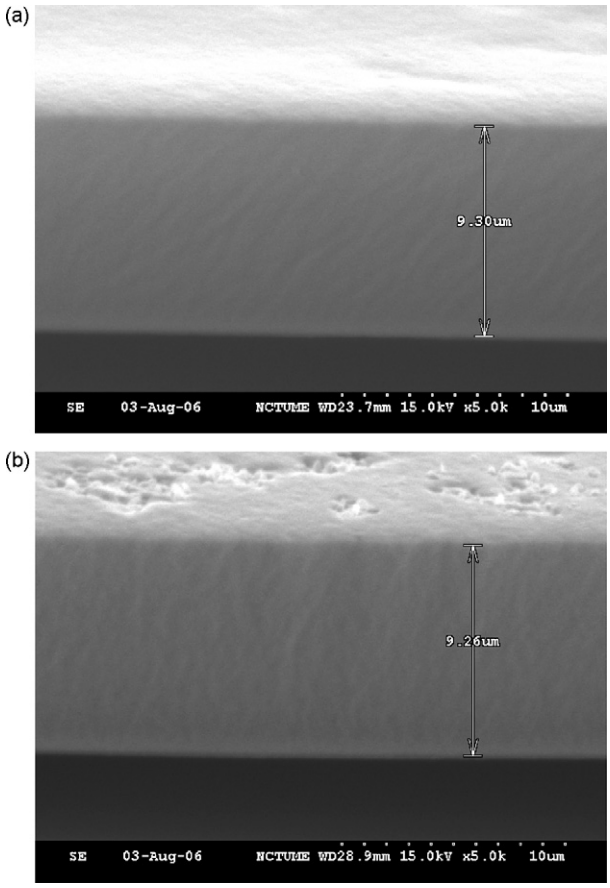

Fig. 8. Side wall SEM pictures of fabricated thermal bimaterial structures: (a) upward type; (b) downward type.

A chip with the thermal bimaterial structure is placed and fixed on piezoelectric shaker which is controlled by waveform generator connected to MEMS motion analyzer (MMA G2™, Etec). The thermal bimaterial structure is driven by an external piezoelectric shaker at destructive resonant frequency of the 5th vibration mode (the first torsion shape) obtained from the modal analysis by the commercial finite-element-analysis (FEA) software ANSYS. For the upward type with 1000 μm length, the 5th resonant frequency is about 108.2 kHz with 0.90 ± 0.05 μm amplitude monitored by an interferometer connected to MMA. Because the delaminated interface has higher influence on the decrement of the resonant frequency of higher order modes, the shift in resonant frequency of the 5th vibration mode is detected to investigate the delamination between interlaminar layers of thermal bimaterial structure. The vibration test result is plotted in Fig. 10 that the resonant frequency is found to be unchanged during 10^9 cycles of continuous vibration. In general, the infinite life of material is defined as no failure happened after 10^6–10^7 cycles in fatigue test [23]. In this study, the test is only performed up to 10^9 cycles, and the measured resonant frequency remains unchanged after 10^9 cycles. This result shows good interlaminar bonding ability between electrodeposited Ni and Ni-diamond nanocomposite since two materials in the thermal bimaterial structure are Ni based.

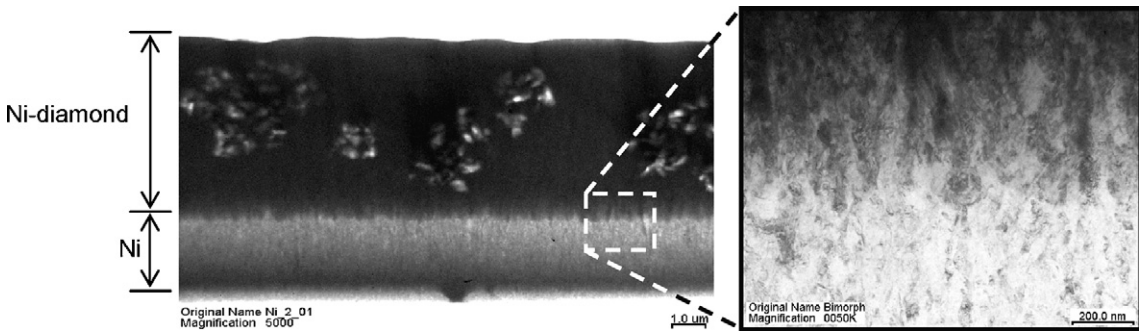

Fig. 9. TEM images of cross section of fabricated thermal bimaterial structure and interface boundary between layers of Ni and Ni-diamond nanocomposite.

4.3. Electro-thermal driven discussion

If the aforementioned bimaterial structures will be used for microactuation application, several design issues should be addressed. In general, electro-thermal microactuators are driven by electric heating, the driving energy Q and the generating temperature change ΔT can be expressed as follows:

$$Q = \frac{V^2\ \Delta t}{R} = mC\,\Delta T \tag{5}$$

and

$$\Delta T = \frac{V^2\,\Delta t}{R \cdot mC} = \frac{V^2\,\Delta t}{\rho(L'/A)\cdot(L'AD\cdot C)} = \frac{V^2\,\Delta t}{\rho DCL'^2} \tag{6}$$

where V, R, Δt, m, L', and A are, respectively, driving voltage, electrical resistance, heating time, mass, total length and cross-sectional area of electro-thermal microactuator. ρ, D, and C are electrical resistivity, density, and specific heat of structural material, respectively. Therefore, while supply voltage is applied to the bimaterial structure, the layer with lower electrical resistivity, i.e. pure Ni layer ($1.59 \times 10^{-5}\ \Omega$ cm, as measured by four-point probe), will have larger temperature change than that of Ni-diamond nanocomposite ($1.87 \times 10^{-5}\ \Omega$ cm, as measured). Since the CTE of Ni is smaller than that of Ni-diamond nanocomposite, the different temperature change to each structural layer will affect the thermal performance in terms of tip deflection due to the neutralization of the thermal elongations of Ni and Ni-diamond nanocomposite. Similarly, this problem also happens to the bimaterial structure of metal/p^+-Si and metal/poly-Si while it is utilized as an electro-thermal microactuator [2,10,13,24]. In order to prevent the occurrence of neutralization, an insulated layer, such as oxide and nitride, is generally used to assure only one heating layer. However, the insulated layer may cause the delamination in the thermal bimaterial structure to reduce the lifetime and reliability of microactuator as mentioned before.

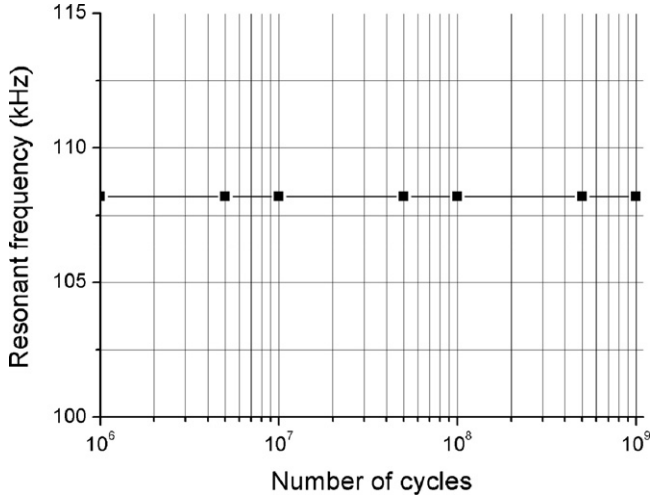

Fig. 10. Resonant frequency detection of thermal bimaterial structure in 10^9 vibration cycles.

Although the neutralization is unavoidable in the Ni/Ni-diamond nanocomposite bimaterial structure without having an insulated layer in between, it could be solved further by controlling the diamond concentration in the Ni-diamond nanocomposite to keep both layers have the same temperature change, i.e. $\Delta T_{Ni-d} = \Delta T_{Ni}$ during electric heating. From Eq. (6), as $\Delta T_{Ni-d} = \Delta T_{Ni}$, it can be found that $\rho_{Ni-d}D_{Ni-d}C_{Ni-d} = \rho_{Ni}D_{Ni}C_{Ni}$. According to the rule of mixture [25], the incorporation of diamond will result in the increase of Ni electrical resistivity and the decrease of Ni density simultaneously. By well controlling the total amount of incorporated nano-diamonds, the multiple of electrical resistivity, density, and heat capacity can be the same to both materials. Thus, the correlation between material properties and nano-diamond concentration requires further investigation for optimal microactuation using the Ni/Ni-diamond bimaterial structure.

5. Conclusions

Thermal bimaterial structures made of electrodeposited Ni and Ni-diamond nanocomposite for CTE mismatch are fabricated successfully to achieve upward and downward out-of-plane displacement easily by controlling plating sequence of electrodeposited Ni and Ni-diamond nanocomposite. Due to the same low process temperature (~50 °C) of electrodeposited Ni and Ni-diamond nanocomposite, the residual thermal stress and initial deformation of fabricated thermal bimaterial structures are small. Since two materials in the thermal bimaterial structure are Ni based, the fabricated thermal bimaterial structure also shows good interlaminar bonding ability between electrodeposited Ni and Ni-diamond nanocomposite. In addition, electrodeposited Ni and Ni-diamond nanocomposite are compatibility with MEMS and CMOS fabrication technologies via a one-step, selective on-chip deposition process at low temperatures (~50–90 °C). Therefore, thermal bimaterial structure made of electrodeposited Ni and Ni-diamond nanocomposite can be integrated into MEMS and CMOS fabrication process for sensor and actuator application.

Acknowledgments

This work is supported by the National Science Council of Taiwan under Grant NSC 95-2221-E-009-012-MY2. Authors would like to express their appreciations to the Nano Facility Center of National Chiao Tung University (NCTU, Taiwan), Instrument Technology Research Center (ITRC, Taiwan), National Chip implementation Center (CIC, Taiwan), National Nano Device Laboratories (NDL, Taiwan), Prof. Pan in National Chin-Yi Technology, Li-Nuan Tsai and Yi-Chia

Lee in Mechanical Engineering Department of NCTU, and Yu-Chiang Chao in Physics Institute of NCTU for providing technical supports and measurement facilities.

References

[1] W.H. Chu, M. Mehregany, R.L. Mullen, Analysis of tip deflection and force of a bimorph cantilever microactuator, J. Micromech. Microeng. 3 (1993) 4–7.
[2] H. Sehr, A.G.R. Evans, A. Brunnschweiler, G.J. Ensell, T.E.G. Niblock, Fabrication and test of thermal vertical bimorph actuators for movement in the wafer plane, J. Micromech. Microeng. 11 (2001) 306–310.
[3] S.H. Lim, J. Choi, R. Horowitz, A. Majumdar, Design and fabrication of a novel bimorph microoptomechanical sensor, J. Microelectromech. Syst. 14 (2005) 683–690.
[4] W. Fang, J.A. Wickert, Comments on measuring thin-film stress using bi-layer micromachined beams, J. Micromech. Microeng. 5 (1995) 276–281.
[5] M.Y. Al Aioubi, V. Djakov, S.E. Huq, P.D. Prewett, Deflection and load characterisation of bimorph actuators for bioMEMS and other applications, Microelectron. Eng. 73–74 (2004) 898–903.
[6] H. Jerman, Electrically activated normally closed diaphragm valves, J. Micromech. Microeng. 4 (1994) 210–216.
[7] C. Hsu, W. Hsu, A two-way membrane-type micro-actuator with continuous deflections, J. Micromech. Microeng. 10 (2000) 387–394.
[8] S. Schweizer, S. Calmes, M. Laudon, P. Renaud, Thermally actuated optical microscanner with large angle and low consumption, Sens. Actuators A 76 (1999) 470–477.
[9] S. Zhou, X. Sun, W.N. Carr, A monolithic variable inductor network using microrelays with combined thermal and electrostatic actuation, J. Micromech. Microeng. 9 (1999) 45–50.
[10] W. Riethmuller, W. Benecke, Thermally excited silicon microactuator, IEEE Trans. Electron Dev. ED-35 (1988) 758–763.
[11] F. Spaepen, A.L. Shull, Mechanical properties of thin films and multilayers, Curr. Opin. Solid State Mater. Sci. 1 (1996) 679–683.
[12] M.T.K. Hou, R. Chen, Effect of width on the stress-induced bending of micromachined bilayer cantilevers, J. Micromech. Microeng. 13 (2003) 141–148.
[13] A. Jain, H. Qu, S. Todd, H. Xie, A thermal bimorph micromirror with large bidirectional and vertical actuation, Sens. Actuators A 122 (2005) 9–15.
[14] S.P. Baker, X. Wang, C.Y. Hui, Effect of nonlinear elastic behavior on bilayer decohesion of thin metal films from nonmetal substrates, J. Appl. Mech. 69 (2002) 407–414.
[15] Y.Q. Fu, H.J. Du, S. Zhang, Sputtering deposited TiNi films: relationship among processing, stress evolution and phase transformation behaviors, Surf. Coat. Technol. 167 (2003) 120–128.
[16] G. Lin, C.J. Kim, S. Konishi, H. Fujita, Design, fabrication, and testing of a C-shape actuator, in: Transducers '95-Eurosensors IX, Stockholm, Sweden, 1995, pp. 416–419.
[17] Y. Zhang, Y. Zhang, R.B. Marcus, Thermally actuated microprobes for a new wafer probe card, J. Microelectromech. Syst. 8 (1999) 43–49.
[18] K.S. Teh, Y.T. Cheng, L. Lin, MEMS fabrication based on nickel-nanocomposite: film deposition and characterization, J. Micromech. Microeng. 15 (2005) 2205–2215.
[19] L.N. Tsai, G.R. Shen, Y.T. Cheng, W. Hsu, Performance improvement of an electrothermal microactuator fabricated using Ni-diamond nanocomposite, J. Microelectromech. Syst. 15 (2006) 149–158.
[20] A.C. Fischer-Cripps, Nanoindentation, 1st edn, Springer, New York, 2002, pp. 27–30.
[21] W. Peng, Z. Xiao, K.R. Farmer, Optimization of thermally actuated bimorph cantilevers for maximum deflection, Nanotechnology 1 (2003) 376–379.
[22] S.S. Kessler, S.M. Spearing, M.J. Atalla, C.E.S. Cesnik, C. Soutis, Damage detection in composite materials using frequency response methods, Composites Part B 33 (2002) 87–95.
[23] J.E. Shigley, C.R. Mischke, R.G. Budynas, Mechanical Engineering Design, 7th edn, McGraw Hill, New York, 2003, pp. 313–315.
[24] C.H. Lin, C.C. Yeh, C.P. Hsu, W. Hsu, Design and fabrication of a cascaded electrothermal bimorph actuator, in: Proceedings of the ASME IMECE'05, Orlando, FL, USA, 2005.
[25] W.D. Callister Jr., Materials Science and Engineering, 4th edn, Wiley, New York, 1996, p. 601.

Biographies

Chia-Sheng Huang was born in Taiwan, in 1979. He received his B.S. and M.S. degrees in the Department of Mechanical Engineering from National Chiao Tung University, Hsinchu, Taiwan, in 2002 and 2004, respectively. He is currently working toward the Ph.D. degree in the Department of Mechanical Engineering, National Chiao Tung University, Hsinchu, Taiwan. His major research interests include the characteristic of nanocomposite material, microactuators, and MEMS technology.

Yu-Ting Cheng was born in Taiwan. He received his B.S. and M.S. degree in Materials Science and Engineering from National Tsing Hua University, Hsinchu, Taiwan in 1991 and 1993, respectively. After his 2-year army service in Taiwan, he went for Carnegie Mellon University, Pittsburgh, PA, and got his second M.S. degree in the same field in 1996. Then he finished his Ph.D. degree in Electrical Engineering from the University of Michigan, Ann Arbor, in 2000. His Ph.D. dissertation is the development of novel vacuum packaging technique for MEMS applications. After his graduation, he worked for IBM Thomas J. Watson Research Center, Yorktown Heights, as a research staff member and was involved in several System on Package (SoP) projects. In 2002, he came back to Taiwan as an assistant professor at the Department of Electronics Engineering in National Chiao Tung University. Since 2005, he has been promoted to be an associate professor. His research interests include the fundamental study of materials for Microsystem integration and MEMS applications, SoP, and the design and fabrication of microsensors and microactuators. He is a member of IEEE, IOP, and Phi Tau Phi.

Junwei Chung was born in Taiwan. He received his M.S. and Ph.D. degrees in the Department of Mechanical Engineering from National Chiao Tung University, Hsinchu, Taiwan, in 2001 and 2007, respectively. His dissertation was entitled "Novel Fabrication Schemes for Non-Silicon-Based Vertical Comb Drive".

Wensyang Hsu received his M.S. and Ph.D. degrees in mechanical engineering from the University of California, Berkeley, in 1990 and 1992, respectively. He is the professor in Mechanical Engineering Department of National Chiao Tung University, Taiwan. His current interests include micro transducers and metal-based surface micromachining.